Articles

QM/MM Study on the Catalytic Mechanism of Benzene Hydroxylation over Fe−ZSM-5

Yoshihito Shiota, Kunihiko Suzuki, and Kazunari Yoshizawa*

Institute for Materials Chemistry and Engineering, Kyushu University, Fukuoka 812-8581, Japan

Received November 8, 2005

The direct conversion of benzene to phenol over Fe−ZSM-5 zeolite is investigated using quantum mechanical/molecular mechanical (QM/MM) calculations on a large model consisting of 683 SiO_2 units (2084 atoms). The active-site model for benzene hydroxylation involves a mononuclear iron-oxo species (Fe^{III}═O) located at the ion-exchangeable Al site of ZSM-5 zeolite. The proposed catalytic cycle is partitioned into four steps: (i) H atom abstraction, (ii) O atom insertion, (iii) phenyl migration, and (iv) phenol release. The decomposition of nitrous oxide plays an important role in the formation of the iron-oxo species and in the avoidance of the unstable Fe^{I} state at the active site. The catalytic reaction occurs on the sextet and quartet potential energy surfaces. The quartet state plays a major role in the course of the reaction, whereas the sextet state lies lower in energy in the entrance channel and in the final stages of the reaction. The QM/MM calculations show that the nanopores of the zeolite framework would decrease the activation barriers in the transition states involved in the reaction pathway and accelerate the exchange of phenol and benzene in the final stages of the reaction. The environmental effect from the zeolite framework promotes the conversion of benzene to phenol.

1. Introduction

Fe−ZSM-5 zeolite is an ion-exchanged zeolite that catalyzes the direct conversion of benzene to phenol using nitrous oxide (N_2O) as an oxidant,[1] as shown in eq 1.

$$C_6H_6 + N_2O \rightarrow C_6H_5OH + N_2 \qquad (1)$$

This reaction is an attractive process that selectively hydroxylates benzene without byproducts, whereas the conventional cumen process yields acetone as a byproduct. Iwamoto and co-workers[2] demonstrated that the conversion of benzene to phenol occurs at 550 °C using N_2O over vanadium oxide silica gel with 71% phenol selectivity. Ono and co-workers[3] reported that phenol is formed from benzene over ZSM-5 zeolite in good yields. Panov and co-workers proposed that the presence of iron impurity in ZSM-5 zeolite plays an important role in the formation of the active species that converts benzene to phenol.[1a] Although this active species, called α-oxygen, is likely to include an iron-oxo species as a catalytic center, structural information about it remains undetermined despite a number of spectroscopic analyses. Samples prepared by aqueous ion exchange show the presence of monoiron and Fe_4O_4 nanoclusters,[4] whereas samples prepared by dry ion exchange show evidence of an oxygen-bridged diiron complex.[5−7] Chen and co-workers[5b] suggested four possible forms for the iron active species of Fe−ZSM-5 zeolite: (i) a monoiron cluster at the tetrahedral site of the zeolite lattice, (ii) a monoiron cluster at the ion-exchangeable Al site, (iii) small iron-oxide nanoclusters, and (iv) an oxygen-bridged diiron complex.

The decomposition of N_2O is a key process for careful understanding of the formation of α-oxygen and the catalytic mechanism. Panov and co-workers[8] suggested on the basis of Mössbauer measurements that α-oxygen is formed on oxygen-bridged dinuclear iron complexes. We proposed from density functional theory (DFT) calculations a mechanism for N_2O decomposition using a monoiron active site model of Fe−ZSM-5,[9] while Yakovlev and co-workers[10] performed theoretical calculations using a diiron complex. Although several theoretical calculations of mononuclear and dinuclear iron complexes have been performed,[9−18] our understanding about the reaction mechanism of the hydroxylation of benzene over Fe−ZSM-5 zeolite is still lacking. We have proposed that benzene hydroxy-

* To whom correspondence should be addressed. E-mail: kazunari@ms.ifoc.kyushu-u.ac.jp.

(1) (a) Panov, G. I.; Sobolev, V. I.; Kharitonov, A. S. *J. Mol. Catal.* **1990**, *61*, 85. (b) Sobolev, V. I.; Panov, G. I.; Kharitonov, A. S.; Romannikov, V. N.; Volodin, A. M.; Ione, K. G. *J. Catal.* **1993**, *139*, 435. (c) Volodin, A. M.; Bolshov, V. A.; Panov, G. I. *J. Phys. Chem.* **1994**, *98*, 7548.

(2) Iwamoto, M.; Hirata, J.; Matsukami, K.; Kagawa, S. *J. Phys. Chem.* **1983**, *87*, 903.

(3) Suzuki, E.; Nakashiro, K.; Ono, Y. *Chem. Lett.* **1988**, 953.

(4) Joyner, R.; Stockenhuber, M. *J. Phys. Chem. B* **1999**, *103*, 5963.

(5) (a) Chen, H.-Y.; Sachtler, W. M. H. *Catal. Today* **1998**, *42*, 73. (b) Chen, H.-Y.; El-Malki, El-M.; Wang, X.; van Santen, R. A.; Sachtler, W. M. H. *J. Mol. Catal. A Chem.* **2000**, *162*, 159.

(6) Marturano, P.; Drozdová, L.; Kogelbauer, A.; Prins, R. *J. Catal.* **2000**, *192*, 236.

(7) Battiston, A. A.; Bitter, J. H.; Koningsberger, D. C. *Catal. Lett.* **2000**, *66*, 75.

(8) Panov, G. I.; Sobolev, V. I.; Dubkov, K. A.; Parmon, V. N.; Ovanesyan, N. S.; Shilov, A. E.; Shteinman, A. A. *React. Kinet. Catal. Lett.* **1997**, *61*, 251.

(9) Yoshizawa, K.; Yumura, T.; Shiota, Y.; Yamabe, T. *Bull. Chem. Soc. Jpn.* **2000**, *73*, 29.

(10) (a) Yakovlev, A. L.; Zhidomirov, G. M.; van Santen, R. A. *J. Phys. Chem. B* **2001**, *105*, 12297. (b) Yakovlev, A. L.; Zhidomirov, G. M.; van Santen, R. A. *Catal. Lett.* **2001**, *75*, 45.

10.1021/om0509591 CCC: $33.50
Publication on Web 05/19/2006

Chart 1

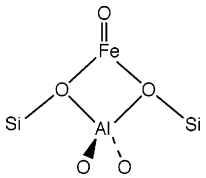

lation reasonably occurs by the α-oxygen species that consists of a mononuclear iron-oxo species (FeO^+).[11] Methane hydroxylation also occurs at the iron active site of Fe−ZSM-5 zeolite. Previously theoretical studies of methane oxidation catalyzed by Fe−ZSM-5 were performed.[11c,13d] In the present work let us turn our attention to the reaction pathway of benzene oxidation by Fe−ZSM-5. The FeO^+ complex that is formed from the reaction between Fe^+ and N_2O in the gas phase is of great interest in considering the catalytic mechanism because it is the simplest oxidation catalyst for the conversion of benzene to phenol.[19] We demonstrated that an FeO^+ complex is formed upon decomposition of N_2O over Fe−ZSM-5 zeolite assuming that the α-oxygen species is located at the ion-exchangeable Al site (the so-called Brønsted acid site).[9] Bell and co-workers[13] proposed that the $[FeO_2]^+$ or $[OFeO]^+$ species is possible as an active species of Fe−ZSM-5 zeolite. However, the oxidation power of iron-peroxo species corresponding to $[FeO_2]^+$ is lower than that of iron-oxo species in general. There is no experimental evidence for the Fe^V state of the $[OFeO]^+$ species over Fe−ZSM-5 zeolite, while the Fe^{II} and Fe^{III} states are observable from Mössbauer measurements.[8] Overweg and co-workers[20] suggested from Mössbauer data that the iron active species of Fe−ZSM-5 zeolite consists of a mononuclear iron complex and that it is rapidly converted between the oxidized Fe^{III} state and the reduced Fe^{II} state at 350 °C. Choi et al.[13c] suggested from EXAFS measurements that an iron atom in the framework of zeolite forms a mononuclear active species at the ion-exchangeable Al site.

Our previous active-site model for the α-oxygen species involves an iron-oxo species (Fe^{III}═O) located at the ion-exchangeable Al site,[11b,c] as shown in Chart 1.

We proposed a reaction pathway for benzene hydroxylation mediated by the mononuclear iron species, as indicated in Figure 1, in which the structure of the ion-exchangeable Al site in the zeolite structure is represented by Z.[11c] In this mechanism the iron-oxo species [FeO]Z is generated by the decomposition of N_2O in the initial stages of the catalytic cycle, and subsequently benzene reacts with [FeO]Z to enter the catalytic cycle, which consists of four steps. (i) The H atom abstraction occurs on the FeO^+ site leading to the hydroxo intermediate $[Fe(OH)C_6H_5]Z$, which involves hydroxo and phenyl groups as ligands. (ii) The decomposition of nitrous oxide causes O atom insertion, resulting in the oxo intermediate $[FeO(OH)C_6H_5]Z$. (iii) A 1,2-phenyl shift occurs to form the phenol complex $[FeO(C_6H_5OH)]Z$. (iv) The release of phenol reproduces [FeO]Z to complete the catalytic cycle for benzene hydroxylation over Fe−ZSM-5 zeolite. The total reaction for the conversion of benzene to phenol with the small model indicated in Chart 1 is 51.0 kcal/mol exothermic at the B3LYP level of theory.

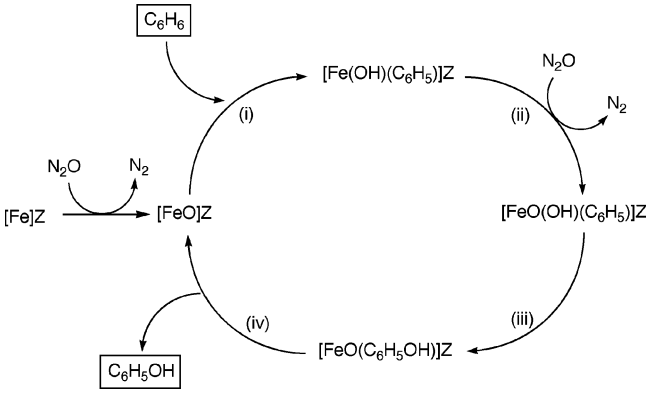

Figure 1. Proposed catalytic cycle for benzene hydroxylation over Fe−ZSM-5 zeolite.

Although the small cluster model built in our previous DFT studies can outline the reaction pathway and energetics in the catalytic cycle of Fe−ZSM-5, no influence of the zeolite framework was taken into account in the small model calculations. In the present study we improve the model to describe the electrostatic and van der Waals interactions between the reaction species and the zeolite framework using a quantum mechanical/molecular mechanical (QM/MM) method. Since the nanopores of ZSM-5 zeolite are expected to play an important role as a reaction field, the QM/MM calculations would give us useful information for the catalytic function of the zeolite framework.

2. Computational Details

QM/MM Model of the Active Site. ZSM-5 zeolite consists of five-, six-, and 10-membered rings with SiO_2 units. The small five- and six-membered rings form the zeolite framework, while the 10-membered rings form the straight channel in the [010] direction and the zigzag channel in the [100] direction. The two channels help the substrate to move from the outside to the active site and the product from the active site to the outside. The present ZSM-5 model consisting of 683 SiO_2 units (2084 atoms) has seven straight and six zigzag channels. Figure 2 shows an optimized QM/MM structure viewed from different angles, in which there are 12 independent sites occupied by an aluminum atom. Although some DFT calculations have been performed on the assumption that the active species is located at the ion-exchangeable Al site of Fe−ZSM-5 zeolite,[9,11b,c,13b,16,17] experimental information about the preferred position of the iron atom is still lacking. We set the iron active species to be located

(11) (a) Yoshizawa, K.; Shiota, Y.; Yamabe, T. *J. Am. Chem. Soc.* **1999**, *121*, 147. (b) Yoshizawa, K.; Shiota, Y.; Yumura, T.; Yamabe, T. *J. Phys. Chem. B* **2000**, *104*, 734. (c) Yoshizawa, K.; Shiota, Y.; Kamachi, T. *J. Phys. Chem. B* **2003**, *107*, 11404. (d) Shiota, Y.; Suzuki, K.; Yoshizawa, K. *Organometallics* **2005**, *24*, 3532.

(12) Stirling, A. *J. Am. Chem. Soc.* **2002**, *124*, 4058.

(13) (a) Ryder, J. A.; Chakraborty, A. K.; Bell, A. T. *J. Phys. Chem. B* **2002**, *106*, 7059. (b) Heyden, A.; Peters, B.; Bell, A. T.; Keil, F. J. *J. Phys. Chem. B* **2005**, *109*, 1857. (c) Choi, S. H.; Wood, B. R.; Bell, A. T.; Janicke, M. T.; Ott, K. C. *J. Phys. Chem. B* **2004**, *108*, 8970. (d) Liang, W.-Z.; Bell, A. T.; Head-Gordon, M.; Chakraborty, A. K. *J. Phys. Chem. B* **2004**, *108*, 4362.

(14) Martínez, A.; Goursot, A.; Coq, B.; Delahay, G. *J. Phys. Chem. B* **2004**, *108*, 8823.

(15) Sang, C.; Kim, B. H.; Lund, C. R. F. *J. Phys. Chem. B* **2005**, *109*, 2295.

(16) Kachurovskaya, N. A.; Zhidomirov, G. M.; van Santen, R. A. *J. Phys. Chem. B* **2004**, *108*, 5944.

(17) Shor, E. A. I.; Shor, A. M.; Nasluzov, V. A.; Vayssilov, G. N.; Rösch, N. *J. Chem. Theory Comput.* **2005**, *1*, 459.

(18) Pantu, P.; Pabchanda, S.; Limtrakul, J. *ChemPhysChem* **2004**, *5*, 1901.

(19) (a) Schröder, D.; Schwarz, H. *Helv. Chim. Acta* **1992**, *75*, 1281. (b) Becker, H.; Schröder, D.; Zummack, W.; Schwarz, H. *J. Am. Chem. Soc.* **1994**, *116*, 1096. (c) Ryan, M. F.; Stöckigt, D.; Schwarz, H. *J. Am. Chem. Soc.* **1994**, *116*, 9565. (d) Schröder, D.; Schwarz, H. *Angew. Chem., Int. Ed.* **1995**, *34*, 1973.

(20) Overweg, A. R.; Crajé, M. W. J.; van der Kraan, A. M.; Arends, I. W. C. E.; Ribera, A.; Sheldon, R. A. *J. Catal.* **2004**, *223*, 262.

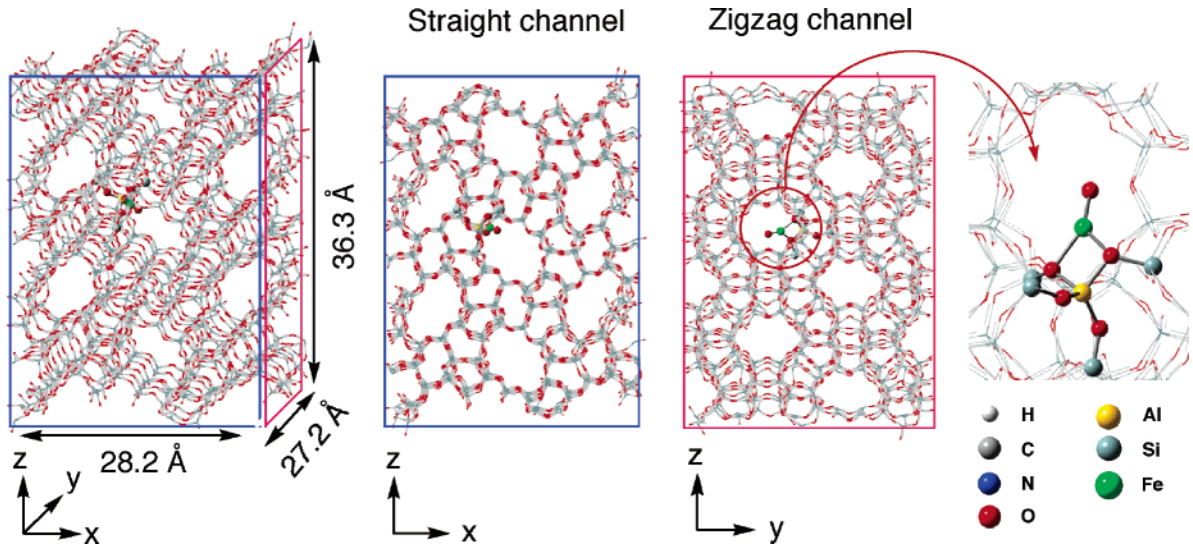

Figure 2. Model of Fe−ZSM-5 zeolite that consists of 2084 atoms. The iron-oxo species is located at the cationic site in the computational model. The QM region is represented by balls and sticks.

in the open space at the intersection of the central straight channel and the central zigzag channel, as shown in Figure 2 (right).

Computational Method. QM/MM calculations were performed using the two-layer ONIOM method[21] in the Gaussian 03 program package (Revision B.03).[22] We assign the iron atom, the aluminum atom, the aluminum-bound $OSiH_3$ groups, and substrate to the QM region and the remaining zeolite framework to the MM region, as indicated in Figure 2. In the QM region we used the B3LYP method[23,24] combined with the D95** basis set[25] for the H, C, N, O, Al, and Si atoms and the Wachters−Hay[26,27] basis set supplemented with one polarization f-function ($\alpha = 1.05$)[28] for the Fe atom. In the MM region we used the universal force field (UFF).[29] Pantu et al.[18] carried out QM/MM calculations for the adsorption energies of N_2O and methane on Fe−ZSM-5 zeolite and reported that the combination of the B3LYP method in the QM region and the UFF method in the MM region provides values consistent with experimental measurements. Rösch and co-workers[17] reported that the ion-exchangeable Al site in the QM region is unaffected by the aluminum loading in the surrounding MM region because the Al/Si ratio of ZSM-5 zeolite is 1/27−1/100 and the interaction between neighboring Al sites is negligible in this Al/Si ratio. Although our QM/MM model contains only one Al atom, this QM/MM calculation is good enough to increase our understanding of the environmental effect of the zeolite framework. The total energy of the system is obtained from three independent calculations within the framework of the ONIOM method, as shown in eq 2.

$$E^{\text{total}} = E^{\text{QM}}(\text{B3LYP}) + E^{\text{All}}(\text{UFF}) - E^{\text{QM}}(\text{UFF}) \quad (2)$$

We analyzed reaction pathways for the possible multistep reactions on the QM/MM potential energy surfaces of the sextet and quartet states. After full geometry optimizations, we reevaluated DFT energies of the QM region only because DFT energies directly reflect the energetics for the chemical reaction under the environmental stress.

3. Results and Discussion

Our proposal on the catalytic cycle is indicated in Figure 1. The mechanisms for benzene hydroxylation by FeO^+ in the gas phase and over Fe−ZSM-5 zeolite are similar in many aspects especially in C−H bond activation. Both reactions are initiated by the formation of a kind of π complex (reactant complex). Subsequent H atom abstraction via the four-centered transition state TS1 results in the formation of the hydroxo intermediate $Fe(OH)(C_6H_5)$. After its formation there is a slight difference between the gas-phase reaction by FeO^+ and the zeolite-mediated reaction. In the gas-phase reaction mediated by FeO^+ a phenyl migration from the iron atom to the oxygen atom results in the formation of the phenol complex $Fe^+(C_6H_5OH)$. The release of phenol finally leads to the bare Fe^+ ion. On the other hand, such a phenyl migration on Fe−ZSM-5 is unlikely to occur in this stage because the formation of Fe^+ is unstable in the condensed phase. Instead of the phenyl migration, we propose that oxygen atom insertion can occur as a result of the decomposition of nitrous oxide on $[Fe(OH)(C_6H_5)]Z$ to result in the formation of the oxo intermediate $[FeO(OH)(C_6H_5)]Z$, in which the formal charge of the iron atom is +5. The oxo

(21) (a) Maseras, F.; Morokuma, K. *J. Comput. Chem.* **1995**, *16*, 1170. (b) Humbel, S.; Sieber, S.; Morokuma, K. *J. Chem. Phys.* **1996**, *105*, 1959. (c) Matsubara, T.; Sieber, S.; Morokuma, K. *Int. J. Quantum Chem.* **1996**, *60*, 1101.

(22) Frisch, M. J.; Trucks, G. W.; Schlegel, H. B.; Scuseria, G. E.; Robb, M. A.; Cheeseman, J. R.; Montgomery, J. A., Jr.; Vreven, T.; Kudin, K. N.; Burant, J. C.; Millam, J. M.; Iyengar, S. S.; Tomasi, J.; Barone, V.; Mennucci, B.; Cossi, M.; Scalmani, G.; Rega, N.; Petersson, G. A.; Nakatsuji, H.; Hada, M.; Ehara, M.; Toyota, K.; Fukuda, R.; Hasegawa, J.; Ishida, M.; Nakajima, T.; Honda, Y.; Kitao, O.; Nakai, H.; Klene, M.; Li, X.; Knox, J. E.; Hratchian, H. P.; Cross, J. B.; Bakken, V.; Adamo, C.; Jaramillo, J.; Gomperts, R.; Stratmann, R. E.; Yazyev, O.; Austin, A. J.; Cammi, R.; Pomelli, C.; Ochterski, J. W.; Ayala, P. Y.; Morokuma, K.; Voth, G. A.; Salvador, P.; Dannenberg, J. J.; Zakrzewski, V. G.; Dapprich, S.; Daniels, A. D.; Strain, M. C.; Farkas, O.; Malick, D. K.; Rabuck, A. D.; Raghavachari, K.; Foresman, J. B.; Ortiz, J. V.; Cui, Q.; Baboul, A. G.; Clifford, S.; Cioslowski, J.; Stefanov, B. B.; Liu, G.; Liashenko, A.; Piskorz, P.; Komaromi, I.; Martin, R. L.; Fox, D. J.; Keith, T.; Al-Laham, M. A.; Peng, C. Y.; Nanayakkara, A.; Challacombe, M.; Gill, P. M. W.; Johnson, B.; Chen, W.; Wong, M. W.; Gonzalez, C.; Pople, J. A. *Gaussian 03, Revision B. 02*; Gaussian, Inc.: Wallingford, CT, 2004.

(23) (a) Becke, A. D. *Phys. Rev. A* **1988**, *38*, 3098. (b) Becke, A. D. *J. Chem. Phys.* **1993**, *98*, 5648.

(24) Lee, C.; Yang, W.; Parr, R. G. *Phys. Rev. B* **1988**, *37*, 785.

(25) Dunning, T. H.; Hay, P. J. In *Modern Theoretical Chemistry*; Schaefer, H. F., III, Ed.; Plenum: New York, 1976; Vol. 3, p 1.

(26) Wachters, A. J. H. *J. Chem. Phys.* **1970**, *52*, 1033.

(27) Hay, P. J. *J. Chem. Phys.* **1977**, *66*, 4377.

(28) Raghavachari, K.; Trucks, G. W. *J. Chem. Phys.* **1989**, *91*, 1062.

(29) Rappé, A. K.; Casewit, C. J.; Colwell, K. S.; Goddard, W. A., III; Skiff, W. M. *J. Am. Chem. Soc.* **1992**, *114*, 10024.

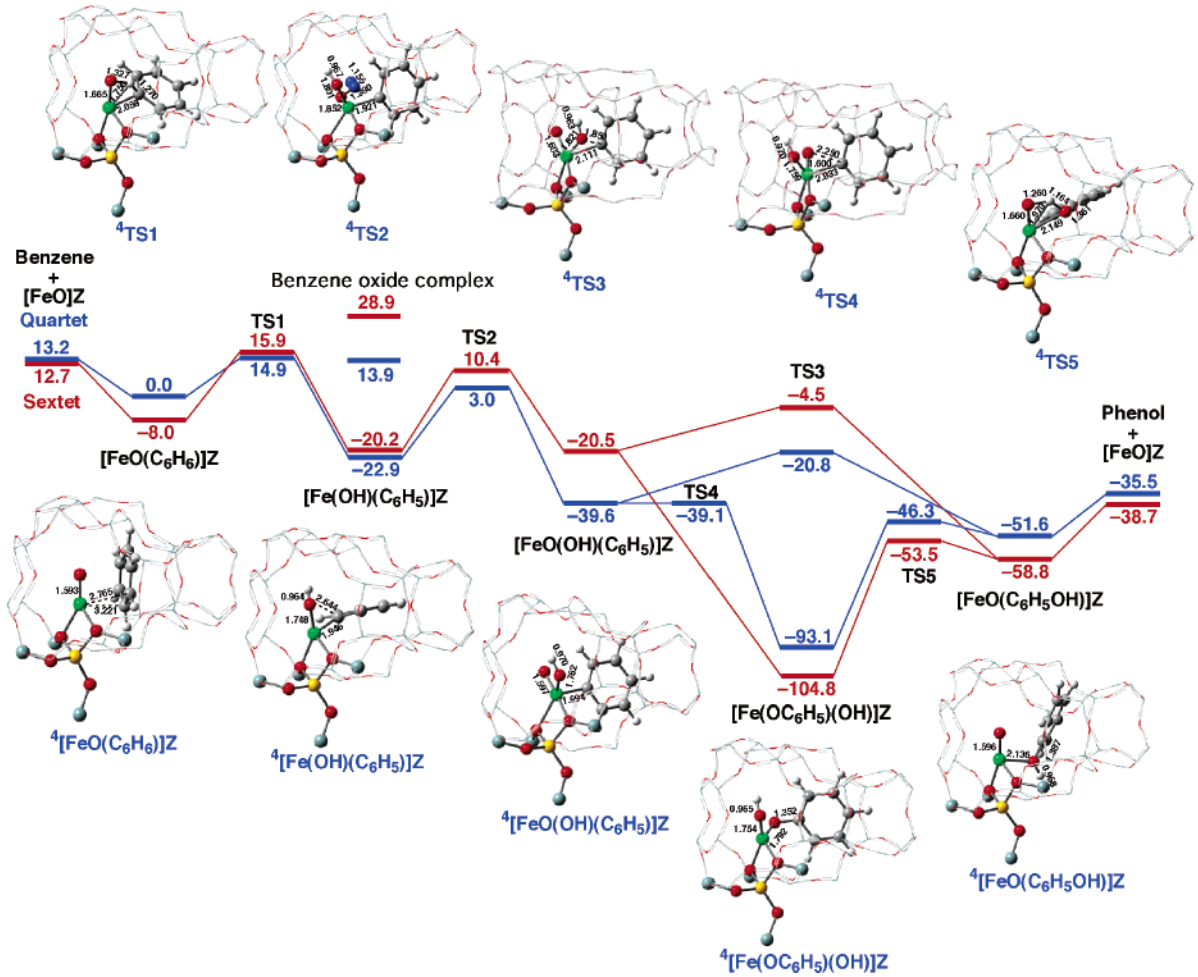

Figure 3. Potential energy diagrams and optimized geometries for benzene hydroxylation over Fe−ZSM-5 zeolite, in which the surrounding zeolite structure is represented by Z. Energies are in kcal/mol and distances in Å.

intermediate undergoes a phenyl migration to form the phenol complex [FeO(C_6H_5OH)]Z, and finally the exchange of phenol and benzene regenerates the initial iron-oxo species [FeO]Z in the catalytic cycle. In this mechanism the formation of Fe^I is avoided in the course of the reaction.

Hydrogen Atom Abstraction. Figure 3 shows optimized structures and relative energies for the H atom abstraction step. In the initial stages of the reaction benzene comes into contact with [FeO]Z to form the reactant complex [FeO(C_6H_6)]Z. It has a weak bond between the iron atom and carbon atoms of the benzene ring. The shortest Fe−C distance in [FeO(C_6H_6)]Z is 2.765 Å in the quartet and 2.542 Å in the sextet. The H atom abstraction occurs via TS1, in which the distances of the C−H and O−H bonds are 1.270 and 1.327 Å, respectively. The phenyl radical is trapped at the iron active center to form the insertion intermediate [Fe(OH)(C_6H_5)]Z. The Fe−O distance increases from 1.593 Å in [FeO(C_6H_6)]Z to 1.748 Å in [Fe(OH)(C_6H_5)]Z via 1.665 Å in TS1, whereas the Fe−C distance decreases from 2.765 Å in [FeO(C_6H_6)]Z to 1.946 Å in [Fe(OH)(C_6H_5)]Z via 2.058 Å in TS1.

The ground sextet state of [FeO(C_6H_6)]Z lies 8.0 kcal/mol below the quartet state, whereas the sextet potential energy surface lies above the quartet one in the vicinity of TS1. Computed energies of TS1 in the sextet and quartet states are 15.9 and 14.9 kcal/mol, respectively, relative to the sextet state of [FeO(C_6H_6)]Z. Therefore the activation barrier decreases from 23.9 kcal/mol in the sextet state to 22.9 kcal/mol in the quartet state if the spin inversion between the two states takes place in a crossing region of the potential energy surfaces. The energy profile of the sextet and quartet potential energy surfaces is a good example for the so-called two-state reactivity concept.[30] Such surface crossing often plays an important role in the course of the oxidation of hydrocarbons by iron-oxo species especially in C−H activation. TS1 of the quartet state lies +5.2 kcal/mol relative to benzene + FeO^+ in the previous small-cluster model,[11c] while this value is +1.7 kcal/mol relative to benzene + [FeO]Z in the present QM/MM model. Thus, the large model calculations suggest that the nanopore of Fe−ZSM-5 assists benzene activation by the iron-oxo species.

Having described the reaction mechanism initiated by the H atom abstraction mechanism, we next consider the oxygen insertion mechanism proposed by Bell and co-workers.[13a,b] According to this reaction mechanism, the reaction pathway consists of two steps. In the first step the reaction initiated by an electrophilic oxygen attack on the benzene ring results in the formation of the benzene oxide complex as a stable intermediate. In the second step the hydrogen migration to the oxygen atom occurs to form the phenol complex. The oxygen insertion in the first step is consistent with no KIE observation with respect to the k_H/k_D values in the oxidation of $C_6H_3D_3$.[31] However, the benzene oxide complex is energetically unfavor-

(30) (a) Fiedler, A.; Schröder, D.; Shaik, S.; Schwarz, H. *J. Am. Chem. Soc.* **1994**, *116*, 10734. (b) Shaik, S.; Danovich, D.; Fiedler, A.; Schröder, D.; Schwarz, H. *Helv. Chim. Acta* **1995**, *78*, 1393. (c) Schröder, D.; Shaik, S.; Schwarz, H. *Acc. Chem. Res.* **2000**, *33*, 139.

(31) Dubkov, K. A.; Sobolev, V. I.; Talsi, E. P.; Rodkin, M. A.; Watkins, N. H.; Shteinman, A. A.; Panov, G. I. *J. Mol. Catal. A* **1997**, *123*, 155.

able, due to disappearance of the resonance energy in the benzene ring, as shown in Figure 3. The benzene oxide complexes in the quartet and sextet states lie 13.9 and 28.9 kcal/mol, respectively, above the reactant complex in the quartet state, while the relative energies of the hydroxo intermediate [Fe(OH)C_6H_5]Z are calculated to be −22.9 kcal/mol in the quartet state and −20.2 kcal/mol in the sextet state. Therefore the B3LYP calculations lead us to conclude that the H atom abstraction mechanism is favored in benzene oxidation over Fe−ZSM-5. No KIE observation most likely indicates that the H atom abstraction is not the rate-determining step in the reaction pathway.

Oxygen Atom Insertion. As mentioned above, the reaction mechanism proposed for Fe−ZSM-5 is different from the one for FeO^+ in the gas phase after the formation of [Fe(OH)(C_6H_5)]Z. Since the Fe^+ ion is very unstable in the condensed phase, we propose that the oxygen atom insertion takes place upon N_2O decomposition to form the oxo intermediate [FeO(OH)(C_6H_5)]Z via TS2.[11c] The decomposition of N_2O gives rise to an increase of the valence state of the iron atom, and therefore the mechanism can avoid the charge state of +1 for the iron atom. Thus, this reaction plays an essential role in forming the iron-oxo species as an oxygen source as well as avoiding the unstable Fe^I species in the catalytic cycle.

Figure 3 shows optimized structures and energy diagrams for the oxygen atom insertion step. The coordination number of the iron atom increases to five in [FeO(OH)(C_6H_5)]Z from four in [Fe(OH)(C_6H_5)]Z. A computed N−O bond distance of 1.390 Å and an Fe−O bond distance of 1.852 Å in TS2 are quite reasonable for the bond cleavage and the bond formation, respectively. A computed Fe−C bond of 1.994 Å in [FeO(OH)(C_6H_5)]Z is slightly longer than 1.946 Å in [Fe(OH)(C_6H_5)]Z. Calculated energies of TS2 are 3.0 kcal/mol in the quartet state and 10.4 kcal/mol in the sextet state relative to [FeO(C_6H_6)]Z in the quartet state. The activation energy for TS2 is 25.9 kcal/mol in the quartet state, whereas in the previous small model the oxygen atom insertion step requires 27.8 kcal/mol. The activation energy for the decomposition of N_2O was estimated from Arrhenius plots of the reaction rate to range from 23 to 37 kcal/mol.[32] Although both previous and present results for TS2 are within the range of the experimental values, the surrounding effect of the ZSM-5 framework slightly decreases the activation energy for TS2. The quartet potential energy surface is 16.7 kcal/mol exothermic in the oxygen atom insertion, while the sextet one is only 0.3 kcal/mol exothermic. Once the spin inversion from the sextet state to the quartet state occurs in TS1, the reacting system will move on the quartet potential energy surface.

Phenyl Migration. The 1,2-phenyl migration from the iron atom to the hydroxo oxygen atom leads to the formation of the phenol complex [FeO(C_6H_5OH)]Z, which releases phenol in the final step to reproduce the initial iron-oxo complex [FeO]Z. Although the phenyl migration looks like a simple process to form a C−O bond, there are two kinds of phenyl migration; one is a direct pathway and the other is a two-step pathway, as shown in Figure 3. The direct pathway also leads to [FeO(C_6H_5-OH)]Z without an intermediate, while the two-step pathway involves the phenoxo intermediate [Fe(OC_6H_5)(OH)]Z.

Figure 3 shows optimized structures and energy diagrams for the two kinds of phenyl migration steps. The direct formation of a phenol complex occurs via a three-centered transition state, TS3. An optimized structure of TS3 has a C−O bond of 1.850 Å, an Fe−C bond of 2.111 Å, and an Fe−O bond of 1.821 Å in the quartet state. These values are quite reasonable as the transition state that connects [FeO(OH)(C_6H_5)]Z and [FeO(C_6H_5-OH)]Z. Calculated activation barriers for this migration step are 18.8 kcal/mol in the quartet state and 16.0 kcal/mol in the sextet state. An optimized structure of [FeO(C_6H_5OH)]Z has two Fe−O bonds of 2.136 and 1.596 Å; the longer Fe−O bond is a coordination bond between the oxygen atom of phenol and the iron active center, and the shorter Fe−O bond corresponds to the iron−oxo double bond.

The first process of the two-step pathway is the formation of [Fe(OC_6H_5)(OH)]Z via TS4, this intermediate being similar to [FeO(OH)(C_6H_5)]Z in the quartet state. An optimized structure of TS4 has a C−O bond of 2.250 Å and an Fe−C bond of 2.033 Å. The geometrical similarity between [FeO(OH)(C_6H_5)]Z and TS4 is consistent with the small activation energy of 0.5 kcal/mol. An optimized structure of [Fe(OC_6H_5)(OH)]Z has a C−O bond of 1.352 Å, corresponding to a C−O double bond. As a result of the C−O bond formation, the Fe−O bond distance significantly changes from 1.597 Å in [FeO(OH)(C_6H_5)]Z to 1.792 Å in [Fe(OC_6H_5)(OH)]Z. The second process of the two-step pathway is a 1,2-hydrogen shift that forms [FeO(C_6H_5-OH)]Z via TS5. This is a four-centered transition state, in which O−H bond cleavage and O−H bond formation occur in a concerted manner. The bond distances for the O−H bond cleavage and formation are 1.260 and 1.164 Å, respectively.

Since the activation energy of the first process is 0.5 kcal/mol in the quartet state, the formation of [Fe(OC_6H_5)(OH)]Z is expected to easily take place. The first process is 53.5 kcal/mol exothermic, while the second process for the 1,2-hydrogen shift requires 46.8 kcal/mol. Although [Fe(OC_6H_5)(OH)]Z is energetically the most stable complex in the catalytic reaction, the thermal energy generated by the first process should be used for the second process. In the sextet state the first process is a barrierless reaction, and thus the second process is important for the formation of [FeO(C_6H_5OH)]Z. The second surface crossing between the sextet and quartet states can occur in the vicinity of [Fe(OC_6H_5)(OH)]Z. Therefore the sextet state becomes the ground state again in [Fe(OC_6H_5)(OH)]Z, while there is no spin inversion in TS3. The energies of TS5 and [FeO(C_6H_5OH)]Z in the sextet state lie below the corresponding energies in the quartet state. Consequently, the phenyl migration is 19.2 and 12.0 kcal/mol exothermic in the sextet state and the quartet state, respectively, relative to [FeO(OH)(C_6H_5)]Z in the quartet state. Calculated activation energies for the phenyl migration step are 18.8 kcal/mol in TS3 and 0.5 kcal/mol in TS4 relative to [FeO(OH)(C_6H_5)]Z in the quartet state. A comparison of the two activation barriers tells us that the two-step pathway is more favorable in the phenyl migration. Note that the two-step pathway is strongly affected by the surface crossing between the quartet state and the sextet state, and therefore the spin inversion is an important process.

Phenol Elimination. Let us next look at [FeO(C_6H_5OH)]Z, which releases phenol to form the final product [FeO]Z. The binding energies thus obtained (E_2) are 20.1 kcal/mol in the sextet state and 16.1 kcal/mol in the quartet state. The binding energies between benzene and [FeO]Z (E_1) are 20.7 kcal/mol in the sextet state and 13.2 kcal/mol in the quartet state. The substitution energies ($E_2 - E_1$) are −0.6 kcal/mol in the sextet state and 2.9 kcal/mol in the quartet state, while the substitution energy in the QM model is 11.6 kcal/mol. This result suggests that the exchange of phenol and benzene is more likely to occur in the zeolite framework.

(32) Sobolev, V. I.; Panov, G. I.; Kharitonov, A. S.; Romannikov, V. N.; Volodin, A. M.; Ione, K. G. *J. Catal.* **1993**, *139*, 435.

Table 1. Computed Binding Energies for Benzene (E_1) and Phenol (E_2) and Activation Energies for TS1 (ΔE_1), TS2 (ΔE_2), TS4 (ΔE_3), and TS5 (ΔE_4) (in kcal/mol) in the Quartet State Using the QM/MM Model and the QM Model (small cluster system)[a]

model	E_1	E_2	ΔE_1	ΔE_2	ΔE_3	ΔE_4
QM/MM	13.2 (20.7)	16.1 (20.1)	14.9 (23.9)	25.9 (30.6)	0.5	46.8 (51.3)
QM[b]	12.2	23.8	17.4	27.8	7.0	33.6

[a] Values in parentheses are the sextet state. [b] QM values from ref 11c.

We finally summarize the environmental effect from the QM model. It is difficult to estimate the environmental effect caused by the interaction between the zeolite framework and the iron-oxo complex. Calculated energies between the QM/MM model and the QM model are summarized in Table 1. In the QM/MM model both the binding energy of phenol and the activation energies for TS1 and TS2 decrease, and therefore the release of phenol, the H atom abstraction, and the decomposition of N_2O are effectively promoted in the zeolite framework. We therefore conclude that the environmental effect from the zeolite framework would effectively accelerate the reaction in the conversion of benzene to phenol.

4. Conclusions

We have presented a theoretical study of the hydroxylation of benzene to phenol over Fe−ZSM-5 zeolite using a QM/MM method to characterize the role of the surrounding zeolite framework. We propose that the active species involves a mononuclear iron-oxo species (Fe^{III}═O) located at the ion-exchangeable Al site of ZSM-5 zeolite. The reaction pathway is partitioned into four steps: (i) the hydroxo intermediate [Fe(OH)(C_6H_5)]Z is formed by the H atom abstraction from benzene, (ii) the decomposition of nitrous oxide occurs on [Fe(OH)(C_6H_5)]Z to lead to the oxo intermediate [FeO(OH)(C_6H_5)]Z, (iii) the phenol complex [FeO(C_6H_5OH)]Z is formed by the phenyl migration that occurs through a direct pathway or a two-step pathway, and (iv) the catalytic process returns to the initial complex [FeO]Z after the release of phenol. The decomposition of N_2O plays an important role in forming the iron-oxo species as well as in avoiding the unstable charge state of +1 for the iron atom. Although this reaction pathway forms the high-valent +5 state for the iron atom, the oxo intermediate [FeO(OH)(C_6H_5)]Z easily transforms into the phenoxo intermediate [Fe(OC_6H_5)(OH)]Z, due to the small activation energy of 0.5 kcal/mol. Thus, the oxo intermediate exists as a short-lived intermediate in Fe−ZSM-5 zeolite. The sextet and quartet potential energy surfaces were characterized in detail at the B3LYP level of theory. After the H atom abstraction the quartet potential energy surface plays a dominant role until the phenyl migration. The quartet and sextet states play an important role in the hydroxylation of benzene over Fe−ZSM-5. The sextet potential energy surface changes into the ground state again in the vicinity of the phenoxo intermediate [Fe(OC_6H_5)(OH)]Z in the reaction pathway. Although the absence of KIE can lead us to conclude that the formation of benzene oxide should take place,[31] we think no KIE observation indicates that the C−H bond activation is not the rate-determining step in the reaction pathway. As shown in Figure 3, the activation energy for the H atom migration via TS5 is greater than that for the C−H bond dissociation via TS1. This computational result is consistent with no KIE observation. The QM/MM calculations demonstrate that the nanopore of the zeolite framework would effectively decrease the activation barriers in the transition states and accelerate the exchange of phenol and benzene in the final stage. The environment effect from the zeolite framework mediated by electrostatic and van der Waals interactions would promote the conversion of benzene to phenol.

Acknowledgment. K.Y. acknowledges the Nanotechnology Support Project of the Ministry of Culture, Sports, Science and Technology of Japan (MEXT), Joint Project of Material Synthesis of MEXT, and CREST of Japan Science and Technology Cooperation for their support of this work.

OM0509591